

RELATIVISTIC QUARK MODEL BASED DESCRIPTION OF LOW ENERGY NN SCATTERING

R. Antalík¹ and V.E. Lyubovitskij²

*Institute of Physics, Slovak Academy of Sciences
842 28 Bratislava, Slovakia*

Abstract

A description of the NN scattering is constructed starting from the π, η, η' pseudoscalar-, the ρ, ϕ, ω vector-, and the $\varepsilon(600), a_0, f_0(1400)$ scalar - meson-nucleon coupling constants, which we obtain within a relativistic quark model. Working within the Blankenbecler-Sugar-Logunov-Tavkhelidze quasipotential dynamics we thus describe the NN phase shifts in a relativistically invariant way. In this procedure we use the phenomenological form factor cutoff masses and the effective ε and ω meson-nucleon coupling constants, only. The comparison of our NN phase shifts to the both empirical data and the Bonn OBEP fit shows good agreement – the ratio of the χ^2 for the present results to the χ^2 for Bonn OBEP description is 1.2.

PACS: 12.40.Aa; 13.75 Cs, 13.75.Gx

¹E-mail address: antalik@savba.sk

²Permanent address: Department of Physics, Tomsk State University, 634055 Tomsk, Russia

1 Introduction

One of main problems in subnuclear physics concerns the structure and interactions of hadrons in terms of their elementary quark and gluon constituents. However, at low energies and small momenta, the traditional description of nuclear forces and nuclear dynamics based on nucleon and meson degrees of freedom appear to give a viable phenomenology of the nuclear reactions and structure [1, 2].

Phenomenologically are nuclear forces understood in terms of meson exchanges. Their long range component, for the first time introduced by Yukawa [3], is generated by a pion exchange. The intermediate range attraction between two-nucleons can be understood in terms of a correlated two pion exchange, usually simulated by a scalar-isoscalar ϵ meson. A repulsive ω meson exchange represents the short range component of two-nucleon forces and the ρ exchange is notably distinctive in the isovector-tensor channel. In such one-boson exchange (OBE) model approach, meson-nucleon coupling constants and form factor cutoffs represent physical parameters, which are to be determined from the best description of the NN scattering data. The conventional relativistically invariant interpretation of the experimental NN phase shifts use such model of the NN forces, see Refs. [1, 4, 5, 6, 7].

The microscopic interpretation of the NN scattering data has mostly rested upon the various nonrelativistic quark models [8, 9, 10]. To preserve the relativistic invariance of the microscopic interpretation, however, one has another possibility, to use the QCD motivated, quantum field theory based models, see, e.g., Refs. [11, 12].

In this paper we investigate a possibility to understand the NN scattering problem starting from a relativistically invariant quark confinement model (QCM) developed at Dubna by Efimov, Ivanov and one of us (V.L.) [13, 14, 15, 16]. Constructing an OBE model of nuclear forces, we use our predictions of meson-nucleon coupling constants that we obtain within the QCM. The form factors we treat but as is usual in a conventional interpretation scheme [1, 7], i.e., we choose their cutoffs to fit the NN phase shifts. This is justified because of the medium renormalization of the meson and nucleon parameters, see, e.g. Ref. [17].

A part of our interpretation scenario – the QCM represents the relativistically invariant effective quantum field theory variant inferred from QCD. Within this scheme are hadrons treated as composed of quarks. The confinement of quarks emerges as in the QCD through nonperturbative gluon vacuum fields. There is no attempt in this model, however, to evaluate the quark confinement, but the S-matrix integration measure itself is conveniently parameterized. This parameterization then allows us to evaluate all quark diagrams representing the meson nucleon interactions.

The processes investigated within this model approach cover the static hadron characteristics, the strong, electromagnetic, and weak dynamical properties of nonflavored, charmed, and bottom mesons and baryons [14, 15, 16, 18, 19]. In all these studies acceptable results have been obtained.

Hence, it shows that the physical picture behind the QCM represents the bulk properties of the hadronic structure, although in the parameterized, nevertheless in the unique way.

In section 2, we will briefly specify the quasipotential dynamics and the meson exchange model of the NN interaction we used here. In section 3, we will briefly review the meson-nucleon coupling constants calculation within QCM. In section 4, we present our results, compare, and discuss them. Section 5 is a conclusion.

2 NN scattering model

To describe the scattering process we work in the framework of the three dimensional quasipotential dynamics using the Blankenbecler-Sugar-Logunov-Tavkhelidze equation [1]. This equation can be written for the R-matrix, which is directly related to the NN phase shifts [20].

It is widely accepted [1, 7] that conventional one-boson exchange model of the NN forces is capable to describe the scattering observables. The NN forces are then given as a sum of the contributions of relevant mesons. As the empirical findings show to describe the low energy NN scattering the pseudoscalar, vector, and scalar meson fields should necessary to be accounted for [1].

In the field theoretical language are meson-nucleon couplings described by the following relativistically invariant Lagrangians for pseudoscalar $\phi^{(ps)}$, scalar $\phi^{(s)}$ and vector $\phi^{(v)}$ meson interactions

$$\mathcal{L}_{ps} = i \sqrt{4\pi} g_{ps} \bar{\psi} \gamma^5 \psi \phi^{(ps)}, \quad (1)$$

$$\mathcal{L}_s = i \sqrt{4\pi} g_s \bar{\psi} \psi \phi^{(s)}, \quad (2)$$

$$\begin{aligned} \mathcal{L}_v = & i \sqrt{4\pi} g_v \bar{\psi} \gamma_\mu \psi \phi_\mu^{(v)} \\ & + i \sqrt{4\pi} \frac{f_v}{4M} \bar{\psi} \sigma^{\mu\nu} \psi (\partial_\mu \phi_\nu^{(v)} - \partial_\nu \phi_\mu^{(v)}), \end{aligned} \quad (3)$$

where g and f describe the vector and tensor couplings of the nucleon field ψ with α meson field $\phi^{(\alpha)}$.

Using Feynman techniques one can obtain the one-boson exchange amplitudes for a particular mesonic field. The pseudoscalar, scalar, and vector meson amplitudes that we need for evaluation of the Blankenbecler-Sugar-Logunov-Tavkhelidze equation in its R-matrix form are explicitly shown in Ref. [6]. The form factors applied at each vertex are taken as

$$F_\alpha(\Delta^2) = \left(\frac{\Lambda_\alpha^2 - m_\alpha^2}{\Lambda_\alpha^2 - \Delta^2} \right), \quad (4)$$

where Λ_α is the cutoff of the α meson of a mass m_α , and $\Delta^2 = (E_{q'} - E_q)^2 - (\mathbf{q}' - \mathbf{q})^2$ is the four-momentum of the exchanged particle [20].

3 Meson-Nucleon Coupling Constant Calculations

3.1 Quark Confinement Model

As the quark confinement model had been developed at Refs. [13, 14, 15], we only briefly review it here. The meson-nucleon (in general the meson-baryon) interaction vertex is within the quark model represented by the Feynman diagram shown in Fig. 1. The quark-hadron vertex is in the quark model described by the interaction Lagrangians of the form

$$\mathcal{L}_H(x) = g_H H(x) J_H(x) , \quad (5)$$

where $J_H(x)$ are quark currents with the quantum numbers corresponding to the considered hadronic field $H(x)$. The renormalized coupling constant g_H for a hadron of a given mass can be obtained from the following compositeness condition

$$Z_H = 1 + \frac{3g_H^2}{(2\pi)^2} \tilde{\Pi}'_H(m_H^2) = 0 , \quad (6)$$

where $\tilde{\Pi}'_H$ is the derivative of the hadronic mass operator.

Let us specify the actual Lagrangian for both types of vertices we have in Fig. 1, i.e., the quark-meson vertex and the quark-baryon vertices. The quark-meson interaction Lagrangian reads

$$\mathcal{L}_M = \frac{g_M}{\sqrt{2}} \sum_{i=1}^8 M_i \bar{q} \Gamma_M \lambda_i q , \quad (7)$$

where q, \bar{q} are the quark, antiquark meson constituting fields, $\bar{q} = (\bar{u}, \bar{d}, \bar{s})$, M_i are the Euclidean mesonic fields relating to the physical mesons in the standard way [15], λ_i are the Gell-Mann matrices, and Γ_M stands instead of $i\gamma^5$ for pseudoscalar mesons $P(\pi, \eta, \eta')$, γ^μ for vector mesons $V(\rho, \omega, \phi)$, and $(I - iH_S\hat{\partial}/\Lambda_q)$ for scalar mesons $S(a_0, f_0, \varepsilon)$. Because of SU(3) breaking, the singlet and octet mesons are mixed as follows

$$\begin{aligned} M &\rightarrow \cos \delta_\Gamma \left(\frac{\bar{u}u + \bar{d}d}{\sqrt{2}} \right) - (\bar{s}s) \sin \delta_\Gamma, \\ M' &\rightarrow -\sin \delta_\Gamma \left(\frac{\bar{u}u + \bar{d}d}{\sqrt{2}} \right) - (\bar{s}s) \cos \delta_\Gamma, \\ M &\equiv (\eta', \omega, \varepsilon); \quad M' \equiv (\eta, \phi, f_0(975)) \end{aligned} \quad (8)$$

where $\delta_\Gamma = \theta_\Gamma - \theta_{I\Gamma}$ and $\theta_{I\Gamma} = 35^\circ$ is the so-called ideal mixing angle. The mixing angles of pseudoscalar and vector mesons are chosen to be equal to $\delta_P = -46^\circ$ and $\delta_V = 0^\circ$, respectively. The scalar meson parameters δ_S , H_S , and m_ε are supposed to be free. Their determination we will comment on in the next subsection.

The SU(3) quark currents with baryon quantum numbers have to be symmetric in respect to the quark field permutation. Since, for the $(1/2)^+$ baryonic octet there are two independent three-quark currents, the quark-baryon interaction Lagrangians read

$$\mathcal{L}_B = \mathcal{L}_{BT} + \mathcal{L}_{BV}, \quad (9)$$

$$\begin{aligned} \mathcal{L}_{BI} &= g_{BI} \bar{B} J_{BI} \\ &= ig_{BI} \bar{B}_j^k R_I^{kj; j_1, j_2, j_3} q_{j_1}^{a_1} q_{j_2}^{a_2} q_{j_3}^{a_3} \varepsilon^{a_1 a_2 a_3} + H.c. \end{aligned} \quad (10)$$

In these expressions $j = (\alpha, m)$; and (a_i, α_h, m_i) are the colour, spin, and flavour indices, respectively. B_j^k are the Euclidean baryonic fields, and matrices $R_I^{kj; j_1 j_2 j_3}$ provide proper quark content of the baryons in the vector or tensor coupling scheme, $I = V, T$.

The meson-nucleon interaction is in a quark model represented through the diagram as in Fig. 1. The typical matrix element corresponding to the process $B \rightarrow B + M$ is proportional to the following expression

$$\begin{aligned} &\int d\sigma_{vac} \bar{B}(x_1) S(x_1 x_3 | B_{vac}) M(x_3) S(x_3 x_2 | B_{vac}) B(x_2) \\ &\times \int d\sigma_{vac'} Tr[S(x_1 x_2 | B_{vac'}) S(x_2 x_1 | B_{vac'})], \end{aligned} \quad (11)$$

where $S(x, x' | B_{vac})$ denotes the quark propagator in the external gluon field B_{vac} and $d\sigma_{vac}$ is the measure of integration over B_{vac} . This highly complex gluon vacuum is supposed to provide quark confinement itself within QCD.

To proceed in evaluation of the expression (11) we make use of the QCM method. The cornerstone of this effective field theory is a prescription for parameterization of the confinement producing gluon vacuum fields [13, 14]. This means that the expression (11) is substituted by the following one:

$$\begin{aligned} &\int d\sigma_v \bar{B}(x_1) S_v(x_1 - x_3) M(x_3) S_v(x_3 - x_2) B(x_2) \\ &\times \int d\sigma_{v'} Tr[S_{v'}(x_1 - x_2) S_{v'}(x_2 - x_1)], \end{aligned} \quad (12)$$

which is the QCM ansatz [13, 14]. In this expression

$$S_v(x_1 - x_2) = \int \frac{d^4 p}{(2\pi)^4 i} \frac{e^{-ip(x_1 - x_2)}}{v\Lambda_q - \hat{p}} \quad (13)$$

is the quark field propagator weighted by the quark confining field parameter v . The model parameter Λ_q determine the confinement range. The indefinite measure $d\sigma_v$ in (12) is defined as

$$\int \frac{d\sigma_v}{v-z} = G(z) = a(-z^2) + zb(-z^2) . \quad (14)$$

The function $G(z)$, the so-called confinement function, is the entire analytical function that decreases faster than any degree of z in the Euclidean direction $z^2 \rightarrow -\infty$. This requirement gives us a possibility to construct the finite theory with confined quarks. Note that this requirement is very general and as a result we can choose the various actual forms of $G(z)$. The confinement function is taken here to be universal, i.e., it is colour and flavour independent, and unique for all quark diagrams determining hadron interactions. As an experience has shown, the only its integral characteristics are important for description of the low energy physics.

To simplify the calculations of the Feynman diagram in Fig. 1, we can substitute the inner two-quark loop by the single propagator, the so-called diquark propagator, Refs. [15]. The meson-baryon vertex of Fig. 1 will then be redrawn to that one shown in Fig. 2. This means that the subdiagram corresponding to the independent two-quark loop

$$\Pi^{\Gamma_1\Gamma_2}(p) = \int \frac{d^4k}{4\pi^2 i} \int d\sigma_{v'} Tr[\Gamma'_1 S_{v'}(p+k) \Gamma'_2 S_{v'}(k)] \quad (15)$$

is substituted by the diquark propagator $D^{\Gamma_1\Gamma_2}$

$$D^{\Gamma_1\Gamma_2}(k) = \frac{d^{\Gamma_1\Gamma_2}}{M_D^2 - k^2} , \quad (16)$$

where M_D is a diquark mass and $d^{\Gamma_1\Gamma_2}$ are coefficients dictated by the symmetry properties. $d^{VT} = -d^{TV} = (ik_\alpha g^{\mu\beta} - ik_\beta g^{\mu\alpha})$. This approximation should fulfill the general requirement - not to break the relation between the baryon electromagnetic vertex and the mass operator, the Ward identity. This identity with the compositeness condition (6) give us needed symmetry properties, see Refs. [15]. Consider the last approximation, the meson-baryon vertex may be written in the form

$$\Lambda_{MNN}(p, p') = \int \frac{d^4k}{\pi^2 i} \int d\sigma_v \Gamma_1 \frac{1}{v\Lambda_q - (\hat{k} - \hat{q})} \Gamma_M \frac{1}{v\Lambda_q - \hat{k}} \frac{d^{\Gamma_1\Gamma_2}}{M_D^2 - (p-k)^2} \Gamma_2. \quad (17)$$

Finally, the transferred momentum ($q = p - p'$) dependent meson-nucleon coupling constants are related to this vertex function as

$$\Lambda_{MNN}(p, p') = T_M G_{MNN}(q^2) , \quad (18)$$

where $T_\pi = \vec{\tau}i\gamma^5$, $T_\eta = T'_\eta = Ii\gamma^5$, $T_{a_0} = \vec{\tau}$, $T_\varepsilon = T_{f_0} = I$, for pseudoscalar and scalar mesons, respectively, and in terms of the vector and tensor form factors

$$\Lambda_{MNN}^\mu(p, p') = T_M \left[\gamma^\mu G_{MNN}(q^2) - i\sigma^{\mu\nu} q_\nu F_{MNN}(q^2) \right] , \quad (19)$$

where $T_\rho = \vec{\tau}$, $T_\omega = T_\phi = I$ for vector mesons. The vector and tensor meson-nucleon coupling constants are the $G_{MNN}(q^2)$ and $F_{MNN}(q^2)$ taken at the zero transferred momentum.

3.2 QCM parameterization

Free parameters of the present QCM version are the parameters of the quark-meson interaction Lagrangian, the confinement ansatz parameters, and the diquark propagator parameter.

As stated above the quark-meson interaction Lagrangian (7) has its free parameters only in the scalar meson sector. These are the derivative term strength H_S , and the mixing angle value δ_S . Both parameters have been determined and thoroughly discussed in Ref. [14].

The confinement ansatz (12-14) free parameters are the coefficients of the confinement functions $a(u)$, $b(u)$ and the light quark confinement parameter Λ_q . As follows from eqs. (12, 14), the confinement functions $a(u)$ and $b(u)$ should be entire analytical functions decreasing sufficiently rapidly in the Euclidean region $Re(u) \rightarrow \infty$. In this paper we take these functions in the simplest forms

$$a(u) = a_0 \exp(-u^2 - a_1 u) , \quad (20)$$

$$b(u) = b_0 \exp(-u^2 + b_1 u) . \quad (21)$$

The coefficients (a_0, a_1, b_0, b_1) , the light quark confinement parameter Λ_q , and the diquark mass M_D have been chosen to fit a convenient set of reference observables [16]. The chosen set of the reference hadronic processes and the resulting QCM values are shown in Table 6 together with the reference empirical data. These results have been obtained with the QCM parameters, which are shown in Table 6.

The obtained parameter set have been used to predict numerous characteristics of hadrons and hadronic processes as magnetic moments of baryons, weak coupling constants, and various decay widths with rather good results in Ref. [16]. That work is in fact a reinvestigation of the same physics as has been studied in the paper [15] using but different – the constant-mass form of the diquark propagator. The application of such form of the diquark propagator has been motivated by the success of the bottom mesons decay studies, where for a heavy-quark propagator the constant-mass propagator has been used.

As one can see in Refs. [14, 15, 18] generally good assessments of the strong, electromagnetic, and weak interactions controlled processes have been acquired within the QCM. It should be said further that after preceding steps we have the effective quark field theory without *free parameters*. Within this frame we can calculate the meson-nucleon coupling constants without additional free parameters too.

4 Results and Discussion

4.1 Introduction

Despite of the fact that the one-boson exchange model is a simplified representation of the NN forces, the effectiveness of this approach is at least at low energies established, see, e.g. Ref. [21]. The strong intermediate range attraction and the strong short range repulsion bring, however, some questions concerning their microscopic understanding. Within OBE models are these NN force properties described by using the ε and ω mesons, to describe the attractive and repulsive forces, respectively [1, 7].

Many studies have been devoted to elaborate understanding of the intermediate range attraction. The studies performed with dispersion relation techniques conclude [22] that a major part of this attraction arises from the correlated two-pion exchanges, which are in turn well approximated by the exchange of the ε meson. The similar results have been obtained in the field-theoretical approach of Ref. [23] and by Bonn group [6] within their full meson exchange model.

There are also other papers, which have studied the intermediate range attraction in a more microscopic way. Thus, using the soliton model Kaiser and Meissner have shown that the inclusion of the pion loops gives the intermediate range attraction with the strength compared to the Paris potential [24]. The new information arises also from a development by Weinberg [25] and others [26], who have recently use a chiral perturbation theory to study the nature of the NN forces. A satisfying qualitative feature, which they have found shows that the uncorrelated two-pion exchange with some of the higher order contact terms provide the intermediate range attraction too. For discussion of the ε meson itself see also very recent development by the Brooklyn group [27]. Other treatments of low-lying scalar mesons can be find also in [28].

It was known for a long time that the short range repulsive force produced by the ω meson exchange partially simulates forces originating from the quark and gluon exchange processes and from heavier vector and tensor meson exchanges also. The understanding of these processes advanced recently also. A qualitative understanding of the short range part of the NN forces has been obtained as produced by the one-gluon exchange in the resonating-group method based quark model [8], or as a “van der Waals’ repulsion” in the chiral bag language [29]. In a more refined model version [10] not only gluons but also Goldstone pions are exchanged between quarks. Their exchange immediately followed by a quark pair exchange add further short range repulsion revealing thus abundance of structures behind the effective OBEP’s ω exchange. As have been discussed [9] such calculations can easily accommodate a repulsive ω exchange using the ω NN coupling compatible with the SU(3) value.

One can see from this discussion that within OBE models we use at least two-mesons, the exchange of which simulate the more complex exchanges too. Consequently, the couplings of these effective exchange fields differ from the couplings of the elementary processes and also from

that ones calculated within the QCD structure level based models. Bearing this in mind, we can go on to discuss our results.

4.2 Included Meson Exchange Fields

The empirical findings show that to describe the low energy NN scattering the pseudoscalar, vector, and scalar meson fields are necessary to generate the exchange forces [1, 7]. To be consistent within the quark model framework we should consider the mesons constructed from the u, d, s quarks. Thus, in the present paper, we take as a set of exchanged mesonic fields the SU(3) pseudoscalar, vector, and scalar mesons. Accordingly, our set of the mesonic fields consists of the π, η, η' pseudoscalars, the ρ, ϕ, ω vectors, and the $a_0, f_0(1400)$ scalar meson fields. Furthermore, we consider the scalar-isoscalar $\varepsilon(600)$ meson also. The $f_0(975)$ meson we do not include in this work because of its coupling constant. The present parameterization of the QCM predicts it to be very small, of about 0.2. The η' meson we should include to be consistent from the quark model point of view, where η and η' are formed in pseudoscalar octet-singlet mixing [30]. The QCM predictions of the meson-nucleon coupling constants, are shown in Table 6. Some of these coupling constants are connected by the SU(3) symmetry relations. These are, the vector couplings for the ρ and ω vector mesons. Further, the ratio of the vector meson Pauli to Dirac coupling constant are $\kappa_\rho = f_{\rho NN}/g_{\rho NN} = (\mu_p - 1) - \mu_n$ and $\kappa_\omega = f_{\omega NN}/g_{\omega NN} = (\mu_p - 1) + \mu_n$.

4.3 OBEP Construction

The construction of our OBE QRBA9 (Quark Relativistic Bosons version A with 9 exchanged fields) model we start out from our QCM predictions of the meson-nucleon coupling constants and typical cutoff masses [7] of the phenomenological form factors (4). Because of the above specified reasons, which are connected with the effectiveness of ε and ω exchanges, we first optimize the εNN and ωNN coupling constants. Afterward, we include to optimization process also the form factor cutoff masses. Parameters of the resulting QRBA9 OBE model are also shown in Table 6.

Concerning the parameter determination procedure the following should be said. As the empirical data we take the phase shift values obtained by Arndt and collaborators [31]. The fitting we span over up to 450 MeV of the nucleon laboratory energy. From a physical viewpoint this may be done because the imaginary parts of the phase shifts in all partial waves are small, except the 1D_2 and 3F_3 waves, in this energy region [1].

4.4 Phase Shifts

Our phase shifts are shown in Figs. 3-4. They are compared there to empirical data and to a phenomenological fit. The referred empirical data are that ones, which we use in our fitting procedure [31]. The results of the mentioned phenomenological fit we calculate from the Bonn

OBEP(B) model [7], commonly regarded as a standard one. Note that this OBE model is affirmed to 325 MeV of the laboratory energy.

As seen, our predictions agree well with the empirical data. To quantify this statement we can say that the ratio of the χ^2 criteria, which we obtain with the QRBA9 model, to that one, we obtain with the Bonn OBEP(B) model [7], is 1.23. Note that because of the coupling to the isobar channel, which is, as it has been shown by Lomon [32], responsible for the resonant behaviour of the 1D_2 and 3F_3 phase shifts, we do not show these phase shifts here (taking them into account the mentioned χ^2 ratio will be 1.80).

Regarding the phase shifts we would like to comment on the behaviour of the $^3S_1 - ^3D_1$ mixing parameter ε_1 only. In a recent phase shift analysis, in which the Basel group has used their newly measured spin correlation parameter in a neutron-proton scattering, they have obtained the value of $\varepsilon_1 = 2.9^0 \pm 0.3^0$ at 50 MeV [33]. The another analysis [34], which includes also the Basel data, reports the value of $\varepsilon_1 = 2.2^0 \pm 0.5^0$ for the same energy. Our prediction is just below 2.6^0 , which is consistent with both mentioned analyses.

To realize the quality of the present phase shifts description, it should be articulated that this should be compared rather to other existing (semi)microscopic results than to the fully phenomenological fit as the Bonn model is. Thus, Fujiwara and Hecht, after their impressive development of the nonrelativistic resonating group method based model, have concluded that they have obtained the semiquantitative fit of the NN phase shifts [35]. Similar results as that ones have been obtained also in Ref. [36]. After a development described in Refs. [10], a semiquantitative fit of the NN scattering data have been obtained in Ref. [37], using but two different couplings for the isoscalar-scalar meson-nucleon vertex.

4.5 Comparison of QCM Predictions with Nonlinear Chiral Effective Lagrangian Predictions and OBEP Model Parameters

Now we compare the QCM coupling constant predictions with that ones obtained within the framework of a nonlinear chiral meson theory in which nucleons emerge as topological solitons (ChSM). Notice that even though accentuating different aspects, both methods, QCM and ChSM, have been deduced from QCD. The ChSM coupling constants have been calculated in two model versions in Ref. [38] with inclusion of the π , ρ , and ω mesons as explicit degrees of freedom. The complete model accounts not only for the chiral anomaly of the underlying QCD through the Wess-Zumino term governing the ω meson coupling to the topological baryon current, as minimal model does, but has also that part of the Wess-Zimino action, which incorporates additional $\pi\rho\omega$ couplings.

Further, we compare theoretical predictions to the meson-nucleon coupling constants from other NN scattering studies. The QCM and both ChSM predictions are together with empirical coupling constants that have been obtained by two leading groups in the low energy NN

scattering phenomenology, namely the Bonn and Nijmegen groups, shown in Table 6.

4.5.1 Pseudoscalar meson-nucleon couplings

The inspection in Table 6 reveals that all QCM coupling constants are lower than ChSM predictions. As seen from the difference between the minimal and complete ChSM models, the mentioned $\pi\rho\omega$ coupling term decrease the π NN coupling by 10 %, bringing it closer to our prediction. Nevertheless, the complete model prediction is still 13 % higher. Note that the much closer result (14.44) have been obtained by Høgaasen and Myhrer [39] within but the cloudy bag model.

A present warm discussion [40, 41, 42] about the π NN coupling constant has appeared on account of the analysis of new π N scattering data by Arndt and coworkers [43]. In that work the VPI&SU group has estimated the charged-pion coupling constant to be 13.31 ± 0.27 being thus in the middle between earlier results of the Nijmegen group. The last group has found first $g^2/4\pi = 13.11 \pm 0.11$ in [44] and later $g^2/4\pi = 13.55 \pm 0.13$ in [45]. Problems arise because these new values of the π NN coupling are much lower than the coupling constant value commonly used for more than a decade, namely 14.28 ± 0.18 , see, Refs. [46, 7]. The primary instruction coming from this development is that the stated errors, being statistical only on the level of 1%, seriously underestimate the real uncertainty [40, 47]. In the last reference it has been shown as well that the minimal value of the $g_\pi^2/4\pi$, which is necessary to describe the deuteron quadrupole moment is 13.65 for the Bonn OBEP [7]. The QCM predicts the π NN coupling constant, which is close to the last value and to the Nijmegen value.

The QCM prediction of the η meson-nucleon coupling is near to the Nijmegen coupling and between the Bonn values. The Nijmegen η' NN coupling is close to our prediction too.

4.5.2 Scalar meson-nucleon couplings

Comparing the QCM predicted a_0 NN coupling constant to phenomenological values obtained in the NN scattering fit, we find that our value is between the Bonn^M model and the Nijmegen model values. All together are but much higher than the Bonn^H value.

Since we do not know other predictions of the $f_0(1400)$ NN coupling constant we do not show this value in Table 6. Note, however, that a decrease of its coupling in comparison with the ε NN coupling shows the mass dependence of the scalar-isoscalar meson-nucleon coupling.

4.5.3 Effective scalar and vector meson-nucleon couplings

As we mentioned already, the intermediate range attractions have been obtained from the correlated two-pion exchange, which has been evaluated with the minimal model Lagrangian of ChSM in Ref. [24]. The resulting two-pion strength between solitons then authors have parameterized by exchange of one-scalar-isoscalar meson with the shown coupling constant. The range

of uncertainty shown there originate in different ad hoc taken pion-loops renormalizing cutoffs. The authors claim, however, that taking into account the full Lagrangian coupling should lead to a higher predicted ε NN coupling and thus perhaps close to the QCM result.

Within the OBE models we use the effective scalar-isoscalar meson as the intermediate range attraction simulating field. Consequently, the constraint on its coupling constant requires of it to has a reasonable value and to be in a strong correlation with the value of the short range repulsive strength, which is generated by the effective ω vector meson-nucleon coupling. Thus, as we explain already, these effective fields simulate the more complex exchanges as well and therefore the values of their couplings cannot be compared to the QCM nor ChSM results.

4.5.4 Vector meson-nucleon couplings

Dirac coupling. The accepted ρ NN vector couplings are about 0.43 ± 0.10 [1], 0.5 [48], which agree with the QCM prediction. These values are compatible with the minimal model prediction but the $\pi\rho\omega$ coupling term of the complete model increase it by additional 47 %. So, the ChSM predictions are 1.36 and 2 times higher then our result.

Our value of the Dirac ρ NN coupling is close to the Bonn^H value, which is but about a factor of 2 lower than Bonn^M one. Note that the Bonn^H OBEP is the same for both isospin channels, like the QRBA9 one, and unlike the Bonn^M set. The Nijmegen OBEP ρ NN coupling is too far from accepted values also, but together with Bonn^M value agree with the prediction of the complete ChSM version.

As QCM is constructed within the SU(3) frame, the QCM ratio of the ω to ρ vector meson couplings is also SU(3) one, namely $g_\omega^2/g_\rho^2 = 9$. Thus the SU(3) expected ω NN vector coupling is about 4. Both ChSM predictions dynamically violate this symmetry being 10.8 and 7.4 for the minimal and complete models, respectively. Nevertheless, ChSM predictions are 1.64 times higher of our value, which is just in the middle between rates we have found for the ρ NN couplings.

Pauli coupling. It is interesting to observe that the ChSM Pauli couplings of the vector mesons have been shifted more closely to the QCM predicted values when $\pi\rho\omega$ coupling term is included also. Thus, the complete model Pauli to Dirac ratio predictions are much close to the empirical findings.

The size of the Pauli coupling constant, which is in common use in OBE models have relied [7] on the old analysis of Ref. [49]. In that paper the value of $\kappa_\rho = 6.1 \pm 0.6$ was obtained for a ratio of the Pauli to Dirac coupling constants. It is known but that the κ_ρ has to be consistent with the empirical value following from a vector meson dominance of a low momentum part of the nucleon electromagnetic form factor. The empirical value of $\kappa_\rho = 3.7$ [1] is consistent with our QCM value $\kappa_\rho = 3.66$ and with the Nijmegen model value $\kappa_\rho = 4.221$.

A recent study of the deuteron properties by Machleidt and Sammarruca [47] shown that to use $\kappa_\rho = 3.7$ in the Bonn^M OBEP $g_\pi^2/4\pi = 13.65$ is needed. This finding is, however, close to

the QCM predictions.

4.6 Form Factors

Expected form factor cutoff masses for different elementary meson-nucleon vertices would not be very different from the well known value of the electromagnetic cutoff mass. The last value is well described in QCM as in ChSM [50] as well as in lattice QCD calculations [51], and quark bag models [9].

The only experimentally studied meson-nucleon vertex is the πNN one. For this vertex, model calculations as well as empirical analyses favour the Λ_π value of about 0.9 GeV. On the other hand, a more indirect process as the NN scattering is, require a much higher value. It thus appears that $\Lambda_{\pi NN}$ needed in the NN scattering is an effective quantity.

As we have mentioned in sect. 1, the expected medium vacuum fluctuations change meson and nucleon propagations [17] and create a variety of different forms of correlations on both structure levels, the QCD as well as the QHD levels. Second, as known, and as it has been recently calculated in Refs. [52, 53], the meson-nucleon interaction is density dependent. Whether this density dependence of a bare meson-nucleon system is effective enough to modify the low energy NN scattering is a priori not known. Further, it is known that the couplings depend also on a type of relativistic equation in use (to observe this one can intercompare OBEP parameters shown in Tables A.1 and A.2 of the Ref. [7]) and on a chosen spectrum of exchanged particles (compare, e.g., different OBE models of the Ref. [21]). Therefore, in the present work we do not intend to solve this form factor problem, but we parameterize it, as all others do also.

Within the present environment, composed of the Blankenbecler-Sugar-Logunov-Tavkhelidze equation and the QRBA9 OBE model, most of used cutoffs are not very certainly determined. The cutoff masses of the η , η' and a_0 mesons may be changed in a wide interval of values without a significant deterioration of the fit quality. The πNN and ρNN vertex cutoffs are on the other hand determined strictly with their correlation measuring -97%.

Although, we do not apply the QCM predicted cutoffs here, it is of specific interest to compare them with other findings, especially for the critical πNN and ρNN vertices. The QCM predicts for the Λ_π and Λ_ρ , the values of 0.88 and 0.60 GeV, respectively. These predictions may be compared to the results of a non-linear chiral meson theory of Ref. [38], where the values obtained for Λ_π and Λ_ρ are 0.86 and 0.93 GeV, respectively. Although the absolute values of the QCM are very different from the QRBA9 model values, Table 6, we find that their ratio is 1.477 comparing to the QRBA9 value of 1.494. The mentioned density dependence of the form factor cutoffs, estimated in [52] for Λ_π and Λ_ρ , represents approximately 20 and 10% reduction at the nuclear density, respectively. On the other hand, a comparison of the QRBA9 cutoffs with the QCM ones shows that the former values are changed by a factor higher than two. This indicate that the density dependence of the form factor cutoffs may be neglected here.

The high $\Lambda_{\pi NN}$ value seems to be nevertheless understandable as an effect produced by vacuum fluctuations in meson exchange currents studied as a renormalization problem in meson theories [17]. As recently has been suggested by Ueda [55] accounts for the role of the $\pi\rho$ and $\pi\varepsilon$ loops explain satisfactorily a difference between the $\Lambda_{\pi NN}$ and $\Lambda_{\pi,(3-body)}$ values. Here, the last $\Lambda_{\pi,(3-body)}$ cutoff, which has a value consistent with our Λ_π value, is the pion-nucleon cutoff one needs to interpret a nuclear three-body problem.

5 Conclusion

In this paper we have investigated the low energy part of the NN scattering relying on the empirical findings that the mesonic degrees of freedom represent a proper way to describe hadron scattering at this energy domain [1]. In this, we have constructed the one boson exchange model using the meson-nucleon couplings predicted by QCM, a model deduced from the QCD. It is to be mentioned that it was not our intention to find a quantitatively competitive description of the NN scattering observables in the present work. Rather, we intend to find a way to understand the NN scattering (generally baryon-baryon scattering) observables having a model parameterized on the quark level only, although it may not be achieved early, and a some guidance should be gathered step by step.

Thus the present NN scattering description is composed of the Blankenbecler-Sugar-Logunov-Tavkhelidze quasipotential equation and the QRBA9 OBE model. Constructing the QRBA9 OBEP we take the meson-nucleon coupling constants as we obtain them as parameter-free predictions of the QCM. The intermediate range attraction and the repulsive short range components of the NN forces we describe as usual through the effective ε and ω exchanges. The cutoff masses we subjugate to fit the empirical phase shifts as common in all models constructed up to now. In result we find that our phase shifts well agree with the empirical data. The ratio of our χ^2 which we obtain with the QRBA9 model to the χ^2 we calculate for the Bonn model [7] is 1.23, what is the unexpectedly good result.

The $\Lambda_{\pi NN}$ and $\Lambda_{\rho NN}$ cutoffs we obtain here are compatible with common OBEP values, however, they are much higher than that ones predicted by the QCM. This observation indicate that the present π and ρ meson exchanges effectively simulate some other processes too. Ueda's explanation of this problem with using vacuum fluctuations in the π exchange channel suggests that the same mechanism may be capable to account for cutoff mass differences in ρ meson exchange channel too.

6 Acknowledgements

We have started this study while working at the LTP JINR, Dubna, Russia. The authors are indebted to G.V. Efimov, M.A. Ivanov and J. Lánik for discussions.

References

- [1] G.E. Brown and A.D. Jackson, *The nucleon-nucleon interaction*, (North Holland, Amsterdam, 1976).
- [2] T.E.O. Ericson and W. Weise, *Pions and nuclei*, (Clarendon, Oxford, 1988).
- [3] H. Yukawa, *Proc. Phys. Mat. Soc.* **17**, 48 (1935).
- [4] M.M. Nagels, T.A. Rijken, J.J. de Swart, *Phys. Rev.* **D17**, 768 (1978).
- [5] M. Lacombe, B. Loiseau, J.M. Richard, R. Vinh Mau, J. Côté, P. Pirès, and R. de Tournell, *Phys. Rev.* **C21**, 861 (1980).
- [6] R. Machleidt, K. Holinde, Ch. Elster, *Phys. Rep.* **149**, 1 (1987).
- [7] R. Machleidt, *Adv. Nucl. Phys.* **19**, 189 (1989).
- [8] M. Oka, K. Yazaki, in *Quarks and Nuclei*, edited by W. Weise (World-Scientific, Singapore, 1984).
- [9] F. Myhrer, J. Wroldsen, *Rev. Mod. Phys.* **60**, 629 (1988).
- [10] K. Shimizu, *Rep. Prog. Phys.* **52**, 1 (1989).
- [11] J.M. Namyslowski, in *Quarks and Nuclear Structure*, edited by K. Bleuler (Springer, Berlin, 1984).
- [12] I. Santhanam, S. Bhatnagar, and A.N. Mitra, *Few-Body Systems* **7**, 141 (1990); S. Chakrabarty, K.K. Gupta, N.N. Singh, and A.N. Mitra, *Prog. Part. Nucl. Phys.* **22**, 32 (1988).
- [13] G.V. Efimov, M.A. Ivanov, *Int. J. Mod. Phys.* **A4**, 2031 (1989).
- [14] G.V. Efimov, M.A. Ivanov, *Sov. J. Part. Nucl.* **20**, 479 (1989).
- [15] G.V. Efimov, M.A. Ivanov, V.E. Lyubovitskij, *Z. Phys.* **C47**, 583 (1990).
- [16] G.V. Efimov, M.A. Ivanov, V.E. Lyubovitskij, Tomsk Scientific Center, Siberian Academy of Science, Preprint 41/90 (1990).
- [17] D. Lurié, *Particles and Fields*, (J. Wiley & Sons, New York, 1968).
- [18] G.V. Efimov, M.A. Ivanov, N.B. Kulimanova, V.E. Lyubovitskij, *Z. Phys.* **C52**, 129 (1991); G.V. Efimov, M.A. Ivanov, V.E. Lyubovitskij, *ibid.* **C52**, 149 (1991); A.M. Ivanov, T. Mizutani, *Phys. Rev.* **D45**, 1580 (1992); A.M. Ivanov, O.E. Khomutenko, T. Mizutani, *ibid.* **D46**, 3817 (1992).

- [19] R. Antalík and V.E. Lyubovitskij, *Few-Body Systems, Suppl.* **5**, 464 (1992); *Czech. J. Phys.* **43**, 747 (1993); *Acta. Phys. Slov.* **43**, 387 (1993).
- [20] K. Erkelenz, R. Alzetta, K. Holinde, *Nucl. Phys.* **A176**, 413 (1971); K. Holinde, K. Erkelenz, R. Alzetta, *ibid.* **A194**, 161 (1971).
- [21] F. Gross, J.W. Van Orden, K. Holinde, *Phys. Rev.* **C45**, 2094 (1992).
- [22] J.W. Durso, A.D Jackson, B.J. Verwest, *Nucl. Phys.* **A282**, 404 (1977); *ibid.* **A345**, 471 (1980); J.W. Durso, M. Saavela, G.E. Brown, A.D. Jackson, *ibid.* **A278**, 445 (1977).
- [23] M.H. Partovi and E.L. Lomon, *Phys. Rev.* **D5**, 1192 (1972); E.L. Lomon, *ibid.* **D14**, 2402 (1976); *ibid.* **D22**, 229 (1980).
- [24] N. Kaiser, U.-G. Meissner, *Nucl. Phys.* **A506**, 417 (1990).
- [25] S. Weinberg, *Phys. Lett.* **B251**, 288 (1990); *Nucl. Phys.* **B363**, 3 (1991); *Phys. Lett.* **B295**, 114 (1992).
- [26] C. Ordonez and U. van Kolck, *Phys. Lett.* **B291**, 459 (1992).
- [27] L.S. Celenza, A. Pantziris, C.M. Shakin, and J. Szweda, Brooklyn College Report, BCCNT 92/102/227 (1992); L.S. Celenza, C.M. Shakin, and J. Szweda, Brooklyn College Report, BCCNT 92/102/228 (1992).
- [28] J. Lánik, *Phys. Lett.* **B306**, 139 (1993); J. Ellis and J. Lánik, *ibid.* **B175**, 83 (1986).
- [29] V. Vento, M. Rho and G.E. Brown, *Phys. Lett.* **B103**, 285 (1981).
- [30] Particle Data Group, K. Hikasa *et al.*, Review of Particle Properties, *Phys. Rev.* **D45**, S1 (1992).
- [31] R.A. Arndt, J.S. Hyslop, L.D. Roper, *Phys. Rev.* **D35**, 128 (1987).
- [32] E.L. Lomon, *Phys. Rev.* **D26**, 576 (1982).
- [33] M. Hammans, C. Brogly-Gysin, S. Burzynski, J. Campbell, P. Haffter, R. Henneck, W. Lorenzon, M.A. Pickar, I. Sick, J.A. Konter, S. Mango, and B. van den Brandt, *Phys. Rev. Lett.* **66**, 2293 (1991).
- [34] R.A.M. Klomp, V.G.J. Stoks, J.J. de Swart, *Phys. Rev.* **C45**, 2023 (1992).
- [35] Y. Fujiwara, K.T. Hecht, *Phys. Lett.* **B171**, 17 (1986); *Nucl. Phys.* **A462**, 621 (1986).
- [36] J. Burger, R. Mueller, K. Tragl and H.M. Hofmann, *Nucl. Phys.* **A493**, 427 (1989).

- [37] K. Bräuer, A. Faessler, F. Fernandez, K. Shimizu, *Nucl. Phys.* **A507**, 599 (1990).
- [38] N. Kaiser, U. Vogl, W. Weise, U.-G. Meissner, *Nucl. Phys.* **A484**, 593 (1988).
- [39] H. Høgaasen, F. Myhrer, *Z. Phys.* **C21**, 73 (1983).
- [40] T.E.O. Ericson, *Nucl. Phys.* **A543**, 409c (1992).
- [41] V. Stoks, R. Timmermans, J.J. de Swart, *Phys. Rev.* **C47**, 512 (1993).
- [42] R. Machleidt, G.Q. Li, *Nucleon-Nucleon Potentials in Comparison: Physics or Polemics?* (University of Idaho Preprint, Moscow, 1993).
- [43] R.A. Arndt, Z. Li, L.D. Roper, R.L. Workman, *Phys. Rev. Lett.* **65**, 157 (1990); *Phys. Rev.* **D44**, 289 (1991).
- [44] J.R. Bergervoet, P.C. van Campen, T.A. Rijken, and J.J. de Swart, *Phys. Rev. Lett.* **59**, 2255 (1987).
- [45] J.R. Bergervoet, P.C. van Campen, R.A.M. Klomp, J.-L. de Kok, T.A. Rijken, V.G.J. Stoks, and J.J. de Swart, *Phys. Rev.* **C41**, 1435 (1990).
- [46] R. Koch and E. Pietarinen, *Nucl. Phys.* **A336**, 331 (1980).
- [47] R. Machleidt and F. Sammarucca, *Phys. Rev. Lett.* **66**, 564 (1991).
- [48] S.-O. Bäckman, G.E. Brown, J.A. Niskanen, *Phys. Rep.* **124**, 1 (1985).
- [49] G. Höhler and E. Pietarinen, *Nucl. Phys.* **B95**, 210 (1975); *ibid.* **B114**, 505 (1976).
- [50] U.-G. Meissner, N. Kaiser and W. Weise, *Nucl. Phys.* **A466**, 685 (1987).
- [51] G. Martinelli and C.T. Sachrajda, *Nucl. Phys.* **B316**, 355 (1989); T. Draper, R.M. Woloshyn, and K.F. Liu, *Phys. Lett.* **B234**, 121 (1990).
- [52] U.-G. Meissner, *Nucl. Phys.* **A503**, 801 (1989).
- [53] Zhi-Xin Qian, Cheng-Gang Su, Ru-Keng Su, *Phys. Rev.* **C47**, 877 (1993).
- [54] K. Holinde, *Phys. Rep.* **68**, 121 (1981).
- [55] T. Ueda, *Phys. Rev. Lett.* **68**, 142 (1992).

Table 1.

Reference hadronic processes. Experimental data taken from [30].

Process	Observable value	Experiment	QCM
$\pi \rightarrow \mu\nu$	f_π (GeV)	0.132	0.131
$\rho \rightarrow \gamma$	$g_{\rho\gamma}$	0.20	0.18
$\pi^0 \rightarrow \gamma\gamma$	$g_{\pi\gamma\gamma}$ (GeV ⁻¹)	0.276	0.287
$\omega \rightarrow \pi\gamma$	$g_{\omega\pi\gamma}$ (GeV ⁻¹)	2.54	2.02
$\rho \rightarrow \pi\pi$	$g_{\rho\pi\pi}$	6.1	6.5
$p \rightarrow p\gamma$	μ_p	2.793	2.798
$n \rightarrow n\gamma$	μ_n	-1.913	-1.864

Table 2.

QCM parameters. The Λ_q , M_D , and m_ϵ are in MeV and δ in degrees.

a_0	b_0	a_1	b_1	Λ_q	M_D	H_S	δ_S	m_ϵ
1.8	2.0	0.6	0.2	400	670	0.55	17	600

Table 3.

The QCM predictions of the meson-nucleon coupling constants, and the QRBA9 OBEP parameters. Numbers in **bold face** were varied during the fitting procedure.

Vertex	QCM	QBRA9	
	$g^2/4\pi(f/g)$	$g^2/4\pi(f/g)$	Λ (MeV)
π NN	13.85	13.85	2110
η NN	3.858	3.858	1000
η' NN	3.065	3.065	1000
ρ NN	0.416 (3.66)	0.416 (3.66)	1410
ϕ NN	1.872	1.872	1410
ω NN	3.740(-0.07)	15.54 (0.0)	2000
ϵ NN	3.620	10.46	2000
a_0 NN	1.996	1.996	1800
$f_0(1400)$ NN	2.062	2.062	2000

Table 4.

Comparison of the QCM with Chiral Soliton Model predictions [38] of meson-nucleon coupling constants and the Bonn^M OBEP(B) version [7], the Bonn^H [54], and the Nijmegen [4] couplings. ^a–the correlated two-pion exchange between two solitons has been simulated by the ε exchange [24].

Vertex	QCM	Chiral Soliton Model		Bonn ^M	Bonn ^H	Nijmegen
	$g^2/4\pi$ (f/g)	Minimal $g^2/4\pi$ (f/g)	Complete $g^2/4\pi$ (f/g)	$g^2/4\pi$ (f/g)	$g^2/4\pi$ (f/g)	$g^2/4\pi$ (f/g)
πNN	13.85	17.3	15.7	14.4	14.4	13.676
ηNN	3.858	—	—	3.0	4.9978	3.433
$\eta' NN$	3.065	—	—	—	—	3.759
$a_0 NN$	1.996	—	—	2.488	0.373	1.632
εNN	3.620	1.4 - 2.3 ^a	—	—	—	—
ωNN	3.740	6.140	6.140	—	—	—
ωNN	(-0.07)	(-0.21)	(-0.07)	—	—	—
ρNN	0.416	0.567	0.835	0.9	0.470	0.795
ρNN	(3.66)	(5.38)	(4.36)	(6.1)	(6.6)	(4.221)
ϕNN	1.872	—	—	—	5.361	0.099

List of Figures

Fig. 1 The meson – three-quark-baryon vertex diagram.

Fig. 2 The meson – quark-diquark-baryon vertex diagram.

Fig. 3 The phase shifts of the NN scattering. The solid lines represent the results obtained with the QRBA9 parameters. The dashed lines refer to the results obtained with the Bonn OBEP(B) model [7]. The circles denote the empirical data of Arndt *et al.*, Ref. [31]. The cross and the square in ε_1 are the empirical data of [33] and [34], respectively.

Fig. 4 The phase shifts of the NN scattering. The notation is the same as in Fig.3.

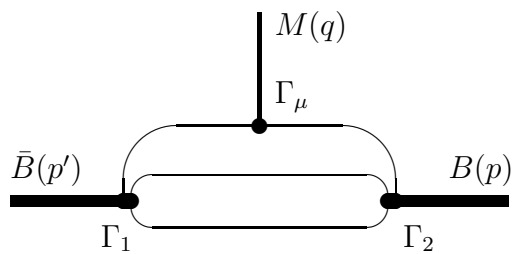


Fig. 1

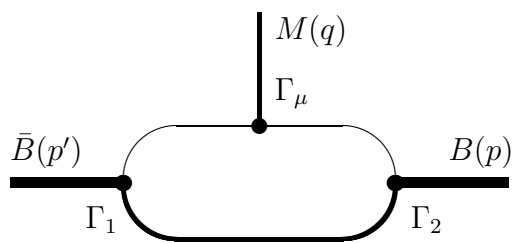


Fig. 2

This figure "fig1-1.png" is available in "png" format from:

<http://arxiv.org/ps/hep-ph/9401280v1>

This figure "fig2-1.png" is available in "png" format from:

<http://arxiv.org/ps/hep-ph/9401280v1>